基于B3样条曲线的复杂焊缝离线示教及跟踪

吴世德， 胡 昊， 于 良
(中国石油大学(北京) 机电工程学院，北京 昌平 102249)


吴世德

摘 要：介绍了一种采用B3样条进行空间复杂弯曲焊缝跟踪的离线样点示教式控制方法. 提出了一种查表方式的改进二分法对插补误差精度进行变步长控制，提高了插补运算的效率和精度. 应用该方法对管道焊接时的相贯线进行了Matlab仿真实现. 结果表明，该示教控制算法有效，可以实现三维弯曲焊缝的示教/再现，最后基于精密焊接的数控系统对三维弯曲焊缝的跟踪控制进行了焊接验证.

关键词：B3样条；插补；改进二分法；焊缝跟踪；示教
中图分类号：TG409 **文献标识码**：A **文章编号**：0253－360X(2011)03－0097－04

0 序 言

由于弧焊时的恶劣环境和焊缝的复杂多变，弧焊实时传感跟踪技术的发展还存在着很大的局限性. 因此，经济实用的焊缝样点示教跟踪技术得到了广泛应用，离线示教跟踪属于开环控制，因此系统稳定可靠，还可以实现复杂弯曲焊缝的弧焊跟踪[1,2].

在样点示教再现过程中，示教效率和插补再现精度取决于采用的轨迹拟合和插值算法，当算法确定后，弯曲焊缝的示教/再现误差主要是由样点个数和插补步长决定. 传统的示教/再现方法在插补运动轨迹时往往采用直线插补或圆弧插补[1,3]. 但是当焊缝为多曲率的空间曲线时，这种插补方法就必须设定大量的示教点才能保证有足够的轨迹再现精度，这对于复杂轨迹的焊接过程的示教，将是一件极为繁琐的工作. 为此，借助于传感视觉装置的辅助示教成为这方面的重要研究内容[1,3,4].

样点示教时，采用具有优良数学特征的三次样条去拟合焊缝轨迹，但其结果要比线性插值估计更近于实际情况. 与一般的三次样条函数相比，B3样条采用参数方程形式，有着优良的曲线平滑性和良好的局部形状可控性，具有复杂平面和空间弯曲曲线的型值点示教能力. 直接的样条插补算法计算复杂，实际应用时多采用等步长查表法来完成[2,5,6]. 采用B3样条进行离线焊缝示教时，示教点少，示教效率高，但是在用于空间弯曲焊缝的再现跟踪时，对于要求的精度来说，因步长不变，有大量的过度插补运算和运动控制，插补效率较低，数据运算量大. 因此研究寻找一种插补精度可控、变步长的快速高效查表算法，减小数据量，避免复杂运算过程和区段条件判断，对于三维以上弯曲焊缝的样条曲线离线示教的跟踪控制有着重要意义.

收稿日期：2009－10－30
基金项目：福建省科技重大专项资助项目(592007HZ0004-1)

1 B3曲线的算法改进

B3作为B样条的一种发展形式，不仅继承了B样条的优点，而且还克服了B样条不通过样点的缺陷. 采用B3样条曲线不但可以实现二维弯曲焊缝的拟合，还可以实现高维空间弯曲焊缝的拟合.

B3样条算法在参数 t(t 为整数时是示教点) 的每个1/3段上寻找满足误差条件的 Δt，然后在该段曲线上利用 Δt 作为步进量对其进行插补. 即拟合得到的样条曲线精确的通过每一个样点. 由于B3样条改进算法是在原有算法的基础上演化出来的，所以首先简要介绍一下B3样条[6].

1.1 B3样条

B3样条曲线是将 i 到 $i+1$ 点间曲线段的参数 $X_i(t)$ 分为三部分，其中每一部分都有一个三次函数形式. 其表达式为

$$X_i(t) = P_{i-1}\cdot h(t+1) + P_i\cdot h(t) + P_{i+1}\cdot h(t-1) + P_{i+2}\cdot h(t-2),\ 0\leqslant t\leqslant 1 \quad (1)$$

式中：$h(t)$ 是B3样条的核函数；P_i 是第 i 个示教点；$h(t)$ 由六部分组成，分别为

$h_1(t)$， $0\leqslant t\leqslant 1/3$； $h_2(t)$， $1/3\leqslant t\leqslant 2/3$.

$h_3(t)$， $2/3 \leqslant t \leqslant 1$； $h_4(t)$， $1 \leqslant t \leqslant 4/3$.

$h_5(t)$， $4/3 \leqslant t \leqslant 5/3$； $h_6(t)$， $5/3 \leqslant t \leqslant 2$.

且 $h(t) \equiv 0$，当 $|t| > 2$ 时，$h_i(t) = h_i(-t)$，$i = 1, 2, 3, \cdots 6$.

根据 B3 样条的要求，$h(t)$ 需要满足 22 个约束条件.

因定义核函数 $h(t)$ 为三次函数形式，a_i, b_i, c_i, d_i 为 $h(t)$ 的系数，即

$$h_i(t) = a_i t^3 + b_i t^2 + c_i t + d_i,\ i = 1, 2, \cdots 6$$

故共有 24 个未知量，现仅有 22 个约束条件，可见 B3 样条核函数并不是唯一确定的. 现选取极小条件 $\min \int_{t=0}^{2} [h''(t)]^2 \mathrm{d}t$，这样得到的 $h(t)$ 函数表达式为

$$h_1(t) = (756t^3 - 1\,116t^2 + 424)/424 \quad (2)$$

$$h_2(t) = (567t^3 - 927t^2 - 63t + 431)/424 \quad (3)$$

$$h_3(t) = (351t^3 - 495t^2 - 351t + 495)/424 \quad (4)$$

$$h_4(t) = (-159t^3 - 1\,035t^2 - 1\,881t + 1\,005)/424 \quad (5)$$

$$h_5(t) = (-645t^3 - 2\,979t^2 - 4\,473t + 2\,157)/424 \quad (6)$$

$$h_6(t) = (246t^3 - 1\,476t^2 + 2\,952t + 1\,968)/424 \quad (7)$$

B3 样条核函数曲线如图 1 所示.

经整理，可得 B3 样条的矩阵表达式，即

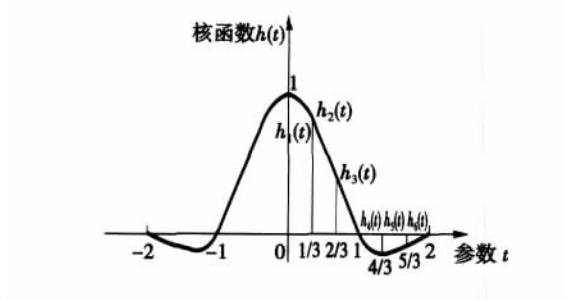

图 1 B3 样条核函数

Fig. 1 B3-spline kernel function

$$X_i(t) = \boldsymbol{T} \cdot \boldsymbol{M} \cdot \boldsymbol{G} \quad (8)$$

式中：$\boldsymbol{T}$ 为关于 t 的行向量；$\boldsymbol{G}$ 为存放四个点的列向量；$\boldsymbol{M}$ 对应着参数 t 在三个区间的系数矩阵. 其中，首尾边界点分别按重复点代入公式. 显然 $X_i(t)$ 与样点 $P_{i-1}, P_i, P_{i+1}, P_{i+2}$ 的位置有关，具有局部形状可控性，且 $X_i(0) = P_i$，$X_i(1) = P_{i+1}$，因此 B3 样条完全通过各个样点，符合焊缝轨迹示教的要求.

1.2 B3 样条算法改进

B3 样条将一段曲线分为三部分，即 $0 \leqslant t \leqslant 1/3$，$1/3 \leqslant t \leqslant 2/3$，$2/3 \leqslant t \leqslant 1$. 计算一段曲线时要计算的内点数应为 3 的倍数. 为简化运算一般可预先计算出核函数 $h(t)$ 在各内点处的值，存于表 1 中，然后依计算点的顺序查表求取 $X_i(t)$，避免公式运算，提高速度. 这种查表法适于等步长的插补运算，缺点是精度可控性不好.

表 1 基于二分法的核函数计算值

Table 1 Kernel calculated value based on dichotomy

t	$t+0/16$	$t+1/16$	$t+2/16$	$t+3/16$	$t+4/16$	$t+5/16$
0	1	0.990 153 76	0.962 356 28	0.919 219 39	0.863 354 95	0.797 374 80
6/16	0.723 858 53	0.645 010 89	0.562 794 81	0.479 169 16	0.396 092 83	0.315 520 09
12/16	0.239 128 83	0.168 168 55	0.103 851 89	0.047 391 50	0	−0.037 403 61
18/16	−0.065 074 99	−0.083 563 46	−0.093 418 34	−0.095 188 93	−0.089 507 48	−0.077 970 11
24/16	−0.062 794 81	−0.046 209 95	−0.030 443 88	−0.017 705 95	−0.009 065 45	−0.003 824 49
30/16	−0.001 133 18	−0.000 141 65	0	—	—	—

与等步长查表法不同，改进算法采用插补精度可控的变步长查表法进行计算，仍采用核函数表达形式预先计算二分点的数值，为了达到插补精度，配合二分法表 1 可以基于 2 的 k 次方无限细分，表 1 给出 $k = 4$ 时 B3 样条核函数的二分表格可供参考. 实际计算的内点数是由在给定插补精度条件下的最佳步长 Δt 决定，搜索方法采用改进二分法. 依照寻优的步长和点数通过指针跳跃查表取得各 $h(t)$，代入式(8) 求得 $X_i(t)$，这种查表算法不需分段考虑，也没有内点数须是 3 的倍数问题，逻辑简单，对于设定的精度条件，插补效率高. 与等步长插补相比，运算次数少，占用的系统时间也更少.

1.3 变步长误差控制方法

插补精度主要取决于插补步长的选择，等步长的插补虽然可以满足插补精度，但插补效率不高. 二分法在步长寻优上具有高效简洁的特点，为了采用二分法进行精度可控的变步长插补，需要对 B3 样条曲线的特性进行分析. B3 样条曲线是以 t 为参数的三次参数方程，其二阶导数为 t 的一次参数方程. 因此，B3 样条曲线的凹凸性只可能出现如图 2

所示三种变化形式的组合.

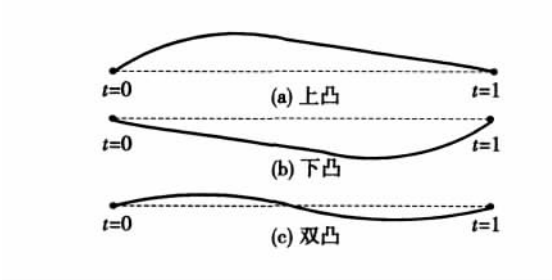

图 2　B3 样条形状图

Fig. 2　B3-spline curve shape mode

对上面三种基本凸凹形式的分析可以发现,使用简单的二分法在图 2c 的情况下容易引起插补精度的误判. 为此,改进的判定准则是在每段曲线上取其 1/4 点、中点、3/4 点到连接该段插补直线的距离(d_1,d_0,d_2) 一起作为插补误差进行判断,看是否满足给定的控制精度,如图 3 所示,如果满足,则插补结束; 如果不满足,则对该曲线进行二分,并选取的 d_1,d_2 较大的一半区间继续应用上述判断方法进行插补误差的判断,直到满足为止.

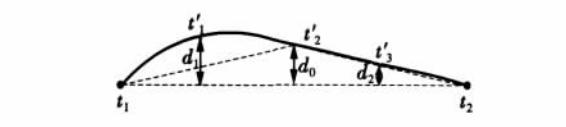

图 3　改进二分法的示意图

Fig. 3　Principle of Improved dichotomy

算法具体实现流程如图 4 所示,改进的二分误差控制方法在给出拟合曲线和控制精度的基础上,可以计算出每段样条曲线满足误差精度的最佳二分插补步长,然后根据最佳步长应用查表法可以得到曲线的插补点.

运动控制时,采用向量分解的方法对插补点之间线性轨迹的焊接速度进行 x,y,z 轴方向上的运动分解,以保证焊接速度的匀速性.

2　仿真结果及分析

焊缝跟踪的效率和精度取决于示教和再现两个过程,即轨迹样点数据的示教拟合和样条曲线运动再现的插补控制.

为了验证 B3 曲线示教及插补误差控制方法的有效性,以直径分别为 200 和 400 mm 的管道相贯线为例进行 Matlab 的仿真分析,设置 16 个样点来示教马鞍形相贯线,拟合的B3样条曲线如图5所

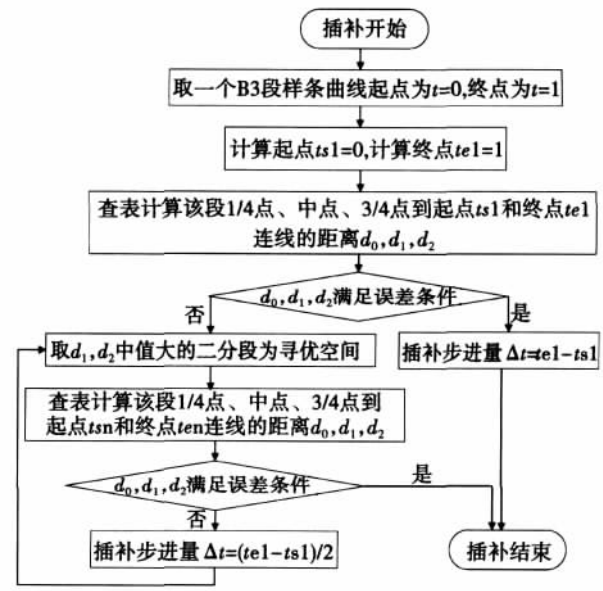

图 4　插补误差控制的算法流程图

Fig. 4　Algorithmic flowchart of Interpolation error control

示. 在等步细分的 N(N = 3 072) 个点分别计算并比较拟合轨迹与实际马鞍线的示教误差,结果如图 6 所示,可以看出基于 B3 样条曲线的插值效果优良,示教效率高,曲线平滑,适于高维的空间曲线样点离散示教. 再现插补的误差控制精度为 0.1 mm,图 7 所示为变步长控制的误差分布趋势图,为达到 0.1 mm 的精度实际插补步数为 160 步.

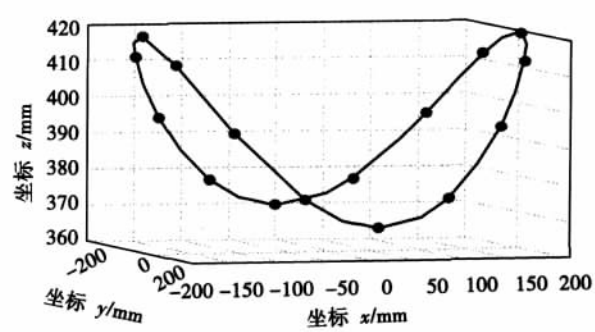

图 5　马鞍形曲线的示教拟合曲线

Fig. 5　Teaching fitting curve of saddle-shape seam

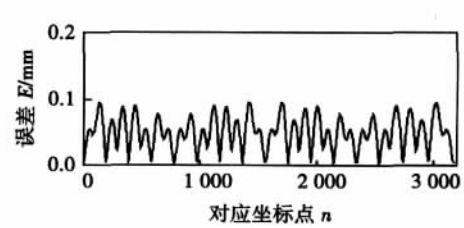

图 6　马鞍形示教误差分布图

Fig. 6　Error distribution diagram teaching fitting error of saddle-shape seam

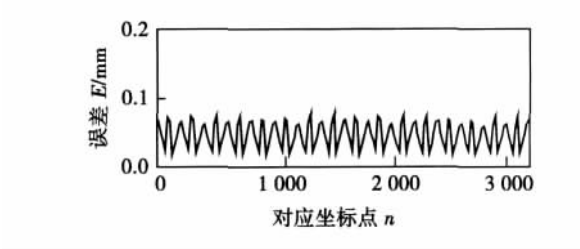

图 7 插补误差趋势图

Fig. 7 Interpolation error trendline of variable step

通过以上结果可以看出，该 B3 样条改进算法不但插补次数少，提高插补精度，而且插补精度严格可控，具有很好的插补效率.

3 焊接试验结果

为验证该方法的可行性，采用熔化极气体保护焊(MIG) 的方法对梯形弯板角接船位焊缝进行示教自动焊接，示教轨迹如图 8 所示，插补精度为 0.1 mm，焊接速度为 420 mm/min，试验结果如图 9 所示，可看出焊缝跟踪良好.

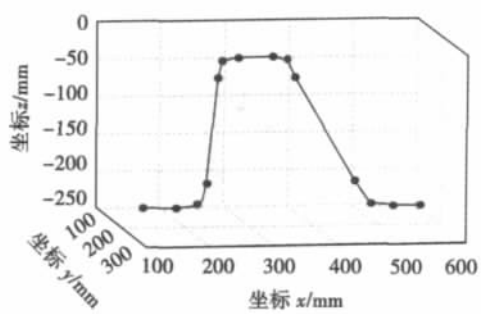

图 8 三维空间曲线焊缝的示教

Fig. 8 3-dimensional curve seam teaching

图 9 弯曲焊缝工件形貌

Fig. 9 Appearance of curve seam works

4 结 论

(1) 通过对基于 B3 曲线插值的焊缝示教跟踪分析和试验表明，此种示教方法能够形成较准确、平滑、较合实际的示教曲线，特别是对于多维空间曲线示教效果优良，示教轨迹可控性好，示教简单效率高，适于手工离散样点的焊缝轨迹示教，对于复杂的空间弯曲焊缝示教跟踪，此方法具有独特的工程实用价值.

(2) 对于 B3 样条曲线的示教焊缝轨迹再现，采用改进二分法对插补误差进行变步长控制的寻优算法计算更简便，又能很好地满足精度控制要求，并实现复杂空间曲线的高效插补. 仿真分析和试验表明此方法无论是插补精度，还是插补效率都能够达到实际应用的要求.

参考文献:

[1] 王加友，陈 刚，朱向运. 示教/再现技术在弧焊跟踪控制系统中的应用[J]. 焊接，1995(2) : 8 - 11.
Wang Jiayou，Chen Gang，Zhu Xiangyun. Application of teaching/playback technique to seam tracking for arc welding [J]. Welding & Joining，1995(2) : 8 - 11.

[2] 王新刚. 多功能自动焊接机床伺服控制技术研究与设备开发[D]. 山东: 山东大学，2007.

[3] 李海超，吴 林，高洪明，等. 应用于遥控焊接的激光机视觉传感辅助遥控示教[J]. 焊接学报，2006，27(5) : 39 - 42.
Li Haichao，Wu Lin，Gao Hongming，*et al*. Technology used in remote welding assisted by laser vision sensing [J]. Transactions of the China Welding Institution，2006，27(5) : 39 - 42.

[4] 蔡春波，张华军，张义顺，等. 基于视觉传感器焊缝跟踪轨迹自示教方法研究[J]. 哈尔滨理工大学学报，2009，14(2) : 95 - 98.
Cai Chunbo，Zhang Huajun，Zhang Yishun，*et al*. Investigation on seam tracking path self-teaching method based on visual sensor [J]. Journal of Harbin University of Science and Technology，2009，14(2) : 95 - 98.

[5] 陈文略，王子羊. 三次样条插值在工程拟合中的应用[J]. 华中师范大学学报(自然科学版) ，2004，38(4) : 418 - 422.
Chen Wenlue，Wang Ziyang. The application of cubic spling interpolation in the project fitting [J]. Journal of Centeral China Normal University(Natural Science) ，2004，38(4) : 418 - 422.

[6] 王洁宁，黄毓瑜. 曲线曲面的 B3 样条拟合[J]. 工程图学学报，1992(2) : 26 - 33.
Wang Jiening，Huang Yuyu. B3-spline fitting for curves & surfaces [J]. Journal of Engineering Graphics，1992(2) : 26 - 33.

作者简介: 吴世德，男，1969 年出生，博士，副教授. 研究方向为焊接自动化、机电系统控制. 发表论文 14 余篇. Email: wusde@ cup. edu. cn

moved reversely 178 mV, the breakdown potential(0.1 V) of the substrate was higher than that of coating(-0.1 V) , which demonstrated the corrosion resistance of the substrate was better than coating.

Key words: plasma cladding; Ni-based alloys; microstructure; corrosion resistance

Microstructure and performance of in-situ synthesis TiN particle reinforced Ni-matrix composite coating WANG Zhenting, ZHENG Wei, ZHOU Xiaohui (College of Materials Science and Engineering, Heilongjiang Institute of Science and Technology, Harbin 150027, China) . p 93 - 96

Abstract: Ni-based composite coating reinforced by TiN particles were prepared on the surface of Q345D steel by means of argon arc cladding technique using Ti, BN and Ni powders as raw materials. The microstructure of the clad layer was observed by scanning electron microscope (SEM) and X-ray diffraction analysis (XRD) . The TiN exhibited sphericity, irregular ellipse and dendrite shapes. The performance of coating were investigated by microhardness test and friction & wear machine. The average hardness of coating was about 840 HV. The argon arc clad composite coating had high hardness and excellent wear resistance under dry sliding wear test conditions.

Key words: argon arc cladding; in-situ synthesis; TiN; composite coating; wear resistance

Complex curved welding seam off-line teaching and tracking based on B3-spline WU Shide, HU Hao, YU Liang (School of Mechanical and Electronic Engineering, China University of Petroleum (Beijing) , Changping, Beijing 102249, China) . p 97 - 100

Abstract: The method of fitting and interpolation for the complex space curved welding seam tracking, depending on off-line samples teaching style by B3-spline curves, was introduced in this paper. In order to improve both accuracy and efficiency of interpolation in seam tracking, the improved dichotomy was proposed for changeable step-size control by the look-up table method. From the Matlab simulation results of pipe welding intersecting lines samples teaching, the methods above could be proved effectively in the process of weld seam tracking control, it provided experimental foundation for developing actual welding control system. Finally, the validity of the method has been verified by welding test.

Key words: B3-spline; interpolation; improved dichotomy; seam tacking; teaching

Friction stir spot welding of AZ31 Mg-alloy YIN Yuhuan[1,2], HU Shengsun[1,2], North T. H.[3], ZHANG Xiaobo[4], SUN Na[5](1. School of Material Science and Engineering, Tianjin University, Tianjin 300072, China; 2. Tianjin Key Laboratory of Advanced Joining Technology, Tianjin University, Tianjin 300072, China; 3. University of Toronto Department of Materials Science and Engineering, Toronto M5S 3E4, Canada; 4. Shanghai Baosteel Casting Corporation, Shanghai 201900, China; 5. Key Laboratory of Automobile Materials of Ministry of Education, Jilin University, Changchun 130025, China) . p 101 - 104

Abstract: The influences of tool rotational speed and dwell time on the mechanical properties of AZ31 friction stir spot welds were investigated. Along with the increase in tool rotational speed, the mechanical properties of AZ31 friction stir spot welds which were made by different tool designs increased first and then decreased. Along with the increase of dwell time, the mechanical properties of AZ31 friction stir spot welds increased first and then kept relatively constant. Bonded width affected the properties of friction stir spot welds significantly. The bigger the bonded widths, the better the properties of the friction stir spot welds were. In addition, the feature of the interface between the upper and the lower sheet also had an important influence on the properties of AZ31 friction stir spot welds.

Key words: friction stir spot welding; mechanical property; tool rotational speed; dwell time; bonded width

Characteristics of welding-brazed joint between Nb-1Zr alloy and 304 stainless steel LI Xin, ZHENG Jianping, ZHAO Jun (China Institute of Atomic Energy, P. O. Box 275-51 , Beijing 102413 , China) . p 105 - 108

Abstract: Electron beam brazing of Nb-1Zr alloy to 304 stainless steel were investigated. It was found that two intermetallic compound layers were formed at brazing interface between stainless steel weld and Nb-1Zr alloy. The reaction layer Ⅰ on Nb-1Zr alloy side was loose organization formed of the Fe_2Nb, while reaction layer Ⅱ on stainless steel weld was formed pillar crystal which was composed of laminated Fe_2Nb and Fe-Cr. The reaction layer Ⅰ brought on frailty of joint and crack in welding. Thickness of reaction layer Ⅰ related to electron beam focus offset, and caused changes in joint strength over 100 MPa. It was not obvious in this experiment that the electron beam current and welding speed caused changes of joint characteristics.

Key words: Nb-1Zr alloy; EBW-brazing; intermetallic compound

Study on microstructure and propertys of TiC-VC particles reinforced surfacing layer prepared by novel twin electrodes welding SHI Hanchao, ZOU Zengda, ZOU Yong, WANG Yufu (Key Lab of Liquid Structure and Heredity of Materials, Ministry of Education, Shandong University, Jinan 250061, China) . p 109 - 112

Abstract: The TiC-VC particles reinforced surfacing layer synthesized from ferrotitanium, ferrovanadium and graphite through metallurgy interaction by novel twin electrodes welding arc had been investigated in this paper. The microstructure and abrasion resistance of surfacing layer were analyzed by XRD、SEM and wear test machine. The results showed that Ti element mainly acted as deoxidize due to the unique twin electrodes welding arc structure, only a small quantity of TiC was formed in the surfacing layer. The main reinforcing phases in surfacing layer were in situ VC, as well as a litter (Ti, V) C phase dispersed in matrix. The surfacing layer had higher surface rigidity of exceeded 55 HRC and better abrasion resistance property. Wear weight loss of surfacing layer was only 1/16 of that of Q235 substrate.

Key words: twin electrodes; TiC-VC; surfacing layer; microstructure; abrasion resistance